crystals

MDPI

Article

Improvement for Interfacial Microstructure and Mechanical Properties of Ti_3SiC_2/Cu Joint Brazed by Ag-Cu-Ti Filler with Copper Mesh

Haiyan Chen [1], Xin Nai [1], Shuai Zhao [1], Decai Lu [1], Zhikang Shen [1,*], Wenya Li [1] and Jian Cao [2]

[1] School of Materials Science and Engineering, Northwestern Polytechnical University, Xi'an 710072, China; hychen@nwpu.edu.cn (H.C.); naixin@mail.nwpu.edu.cn (X.N.); shuaizhao@mail.nwpu.edu.cn (S.Z.); decailu@mail.nwpu.edu.cn (D.L.); liwy@nwpu.edu.cn (W.L.)

[2] School of Materials Science and Engineering, Harbin Institute of Technology, Harbin 150001, China; cao_jian@hit.edu.cn

* Correspondence: zhikangshen@nwpu.edu.cn

Abstract: Ti_3SiC_2 ceramic and copper were successfully vacuum brazed using Ag-Cu-Ti filler and Ag-Cu-Ti filler with copper mesh, respectively. In this study, the effects of copper mesh and brazing parameters on the interface microstructure and mechanical properties of the joints were systematically studied. The results revealed that the typical interfacial microstructure of joint was Ti_3SiC_2 ceramic/Ti_5Si_3 + TiC + Ti_2Cu + Ti_3Cu/Ag (s, s) + Cu (s, s)/eutectic Ag-Cu + TiSiCu/Cu. A maximum shear strength of joint obtained at a brazing temperature of 870 °C and a holding time of 10 min can reached up to 66.3 ± 1.2 MPa, which was 34.7% higher than that without copper mesh. The improvement of mechanical property was attributed to the extraordinary plasticity of copper mesh, which reduced the residual stress caused by the difference in the coefficient of thermal expansion at the interface of joints. As the brazing temperature and holding time further increased, the shear strength of joints decreased due to the excessively thick reaction layer of intermetallic compounds.

Keywords: Ti_3SiC_2 ceramic; brazing; copper mesh; microstructure; mechanical properties

Citation: Chen, H.; Nai, X.; Zhao, S.; Lu, D.; Shen, Z.; Li, W.; Cao, J. Improvement for Interfacial Microstructure and Mechanical Properties of Ti_3SiC_2/Cu Joint Brazed by Ag-Cu-Ti Filler with Copper Mesh. *Crystals* **2021**, *11*, 401. https://doi.org/10.3390/cryst11040401

Academic Editors: Tianhao Wang, Bharat Gwalani, Jiahao Cheng, Michael Frank, Yunqiang Zhao, Junmiao Shi and Shujun Zhang

Received: 14 March 2021
Accepted: 4 April 2021
Published: 10 April 2021

1. Introduction

Ti_3SiC_2 ceramic is widely used in the production of conductive components and corrosion-resistant electrodes owing to its outstanding electrical conductivity, thermal conductivity, and workability comparable to the graphite [1,2]. However, it is still difficult to manufacture large-scale Ti_3SiC_2 ceramic and process complex-shaped components, which greatly limits the application of Ti_3SiC_2 ceramic. In order to expand the application of Ti_3SiC_2 ceramic, it has become an important way to obtain the composite components of Ti_3SiC_2 ceramic and metal materials by joining technology [3]. Compared with other metals or alloys, pure copper is usually joined with Ti_3SiC_2 ceramic to form composite components in the field of electrical conductivity and wear resistance due to its excellent conductivity, high fracture toughness, and good workability [4,5]. However, the great differences in physical and chemical properties between Ti_3SiC_2 ceramic and pure copper are still the barriers for the manufacturing and application of Ti_3SiC_2/Cu composite component [6,7]. Therefore, it is necessary to find an optimal joining technology to manufacture the composite components.

At present, several joining technologies including laser welding, electron beam welding, diffusion bonding, adhesive bonding, transient liquid phase bonding, and vacuum brazing have been developed to obtain the ceramic-metal assemblies [8–15]. Compared with other joining methods, vacuum brazing is a relatively precise and reliable method for joining dissimilar materials, especially for ceramic and metals. However, obtaining a ceramic/metal brazed joint with good mechanical properties often suffers from two problems. One is the poor wettability of liquid metal-based brazing fillers on the surface

of ceramics substrate. Yan et al. [16,17] adopted ultrasonic-assisted brazing technology to greatly promote the wetting and spreading of liquid fillers on the surface of SiC ceramic substrate. Feng et al. [18] studied the interfacial microstructure and morphology of the ZrC/SiC-Ti_6Al_4V joint brazed by Ag-Cu-Ti filler metals, which indicated that Ti element greatly promoted the metallurgical bonding of ceramic with fillers. Xiong et al. [19] developed a new type of Pd-based active fillers to successfully realize the brazing of Ti_3Al and nickel-base superalloy. Waetzig et al. [20] studied the influence of the brazing paste composition on the wetting behavior. To date, the wettability of metal-based fillers on the surface of ceramic has been effectively improved by multiple methods.

The other problem that has not been solved is the concentration of residual stress at the interface of ceramic/metal joint. The residual stress will inevitably occur in the brazed joint during the cooling process due to the mismatch of CTE among ceramic-based materials, metal-based materials, and fillers [21–24]. In order to relieve the concentration of residual stress and promote the strength and toughness of brazed joint, several methods have been introduced to the brazing of ceramics and metals, including composite fillers [25–27], surface processing [28–30], metal foil interlayer [31–34], mesh metal [35–38], and so on. However, adding ceramics particles into fillers to make composite fillers leads to very complex interface products, surface processing increases the pre-welding workload greatly, and the new interface introduced in metal foil interlayer method is a potential disadvantage to promote the propagation of cracks. Compared with other methods, high-plastic metal mesh is a more effective and easy-making method to release the residual stress. Sun et al. [39] reported that Al_2O_3 ceramic was brazed to 1Cr18Ni9 by Ni foam. When using Ni foam as the interlayer, the shear strength of the joints was 72.1 MPa. Zaharinie et al. [40] introduced a porous Cu/Ni composite as an interlayer to braze sapphire ceramic and Inconel 600 alloy for pressure sensor applications. Tian et al. [41] introduced an interlayer of Cu foam to increase the brazing strength of the joints, which reached up to 121 MPa, 460% higher than that without Cu foam interlayer. A composite interlayer of carbon-covered Cu foam was found helpful for the formation of TiC when brazing C/C composite and Nb [42]. Singh et al. [43] used a SiC-coated foam to achieve the graphite foam/titanium joints successfully.

However, there are a few reports on the release of residual stress in Ti_3SiC_2 ceramic/copper brazed joints, especially the metal mesh method. In the studies on metal mesh method, it is still uncommon to brazed the ceramic/metal joint using the metal mesh with the same composition as the metal base material, and the influence of metal mesh on the interface microstructure and mechanical properties of joints also needs to be investigated. In this study, the brazing of Ti_3SiC_2 ceramic and pure copper was successfully achieved using Ag-Cu-Ti fillers with and without copper mesh, respectively. In this paper, the effects of brazing parameters and copper mesh on interfacial microstructure and mechanical properties of joints were surveyed and discussed.

2. Experimental Materials and Methods

Ti_3SiC_2 ceramic substrate was made by spark plasma sintering and pure copper was commercially available. Ti_3SiC_2 ceramic was cut into 10 mm × 10 mm × 2 mm pieces by wire EDM for metallographic analysis and mechanical property test. While the pure copper was cut into 10 mm × 10 mm × 2 mm and 120 mm × 10 mm × 10 mm pieces for metallographic analysis and mechanical property test, respectively. All Ti_3SiC_2 ceramic and copper surfaces to be brazed were ground by SiC paper up to grit 2000 and polished with 1.5 μm diamond paste. The interlayer used in this study was a composite filler of Ag-27.5Cu-2Ti power with and without copper mesh, and the parameters of filler power and copper mesh are listed in Table 1. The copper mesh was cut into the size matching to the ceramic piece. Then the ceramic, pure copper, and copper mesh were ultrasonically cleaned for 10 min.

Table 1. Parameters of filler power and copper mesh.

Material	Chemical Composition (wt.%)	Purity (wt.%)	Particle Size or Porosity	Melting Point (°C)
Metal power filler	Ag-27.5Cu-2Ti	>99.9	50 μm	800–820
Metal mesh	Cu	>99.9	≈85%	1083

The ball-milled Ag-27.5Cu-2Ti powder filler was mixed with a commercially available brazing paste to prepare the paste-like filler, which was coated on the surface of the Ti_3SiC_2 ceramic sample for 100–200 μm. Subsequently, the copper mesh was placed and pressed on the paste-like filler, and then the pure copper piece was placed on the composite filler interlayer, which presented a sandwich structure as shown in Figure 1. In this study, the brazing temperature range was selected to be 840–900 °C and the holding time was set to 5–30 min. The detailed brazing process parameters are shown in Figure 2. The number of samples used to test mechanical properties under each brazing parameter was five.

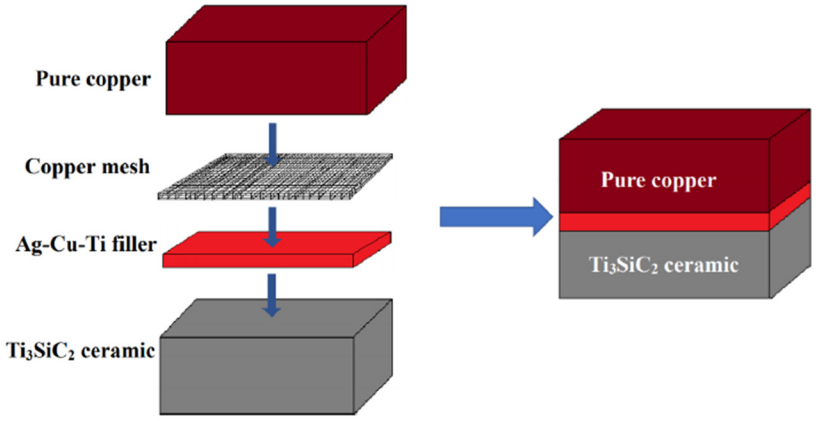

Figure 1. Assembly scheme of brazing sample.

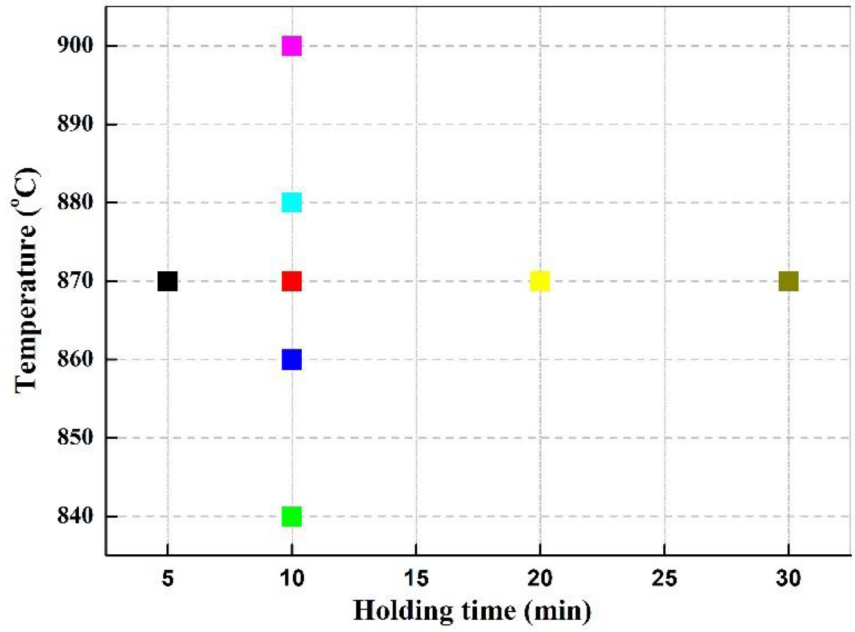

Figure 2. Brazing process parameters of Ti_3SiC_2 ceramic/copper joints.

After the brazing, the samples were cut and polished to make metallographic samples for observing the interfacial microstructure and analyzing the chemical composition of brazed joints by scanning electron microscope (SEM, Verios G4, FEI, USA) equipped with

energy-dispersive spectrometer (EDS, Aztec, Oxford, UK). In addition, the products at the interface were analyzed using X-ray diffraction analyzer (XRD, X-Pert PRO, PANalytical B.V., The Netherlands). In this study, the shear strength was used to characterize the mechanical properties of brazed joints. A universal testing machine was used to test the mechanical properties of the Ti_3SiC_2 ceramic/copper brazed joints. The self-made fixture in the shear strength test and the sample placement form are shown in Figure 3. The moving speed of the indenter in the shear test is 0.5 mm/min, and the shear strength is the average values of five samples.

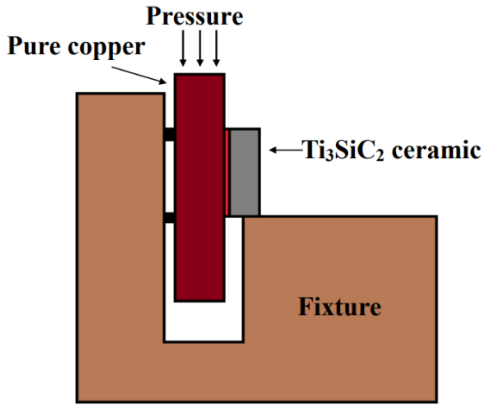

Figure 3. Schematic diagram of shear strength test.

3. Results and Discussion

3.1. The Interfacial Microstructure and Reaction Mechanism of Ti_3SiC_2/Cu Joint

Figure 4a,b shows the interfacial microstructure of Ti_3SiC_2 ceramic/pure copper joint brazed using Ag-Cu-Ti without and with copper mesh at 880 °C for 10 min. As shown in Figure 4, both types of Ti_3SiC_2/Cu joints were brazed tightly. For Ti_3SiC_2/Ag-Cu-Ti/Cu joint, most of the interface was well brazed except for a few voids and cracks, while there were no obvious defects such as voids and cracks at the interface of Ti_3SiC_2/Ag-Cu-Ti + Cu mesh/Cu joint. For both types of joints, the diffusion and reaction in the ceramic side were obvious, and the thickness of the diffusion and reaction layer in the Ti_3SiC_2/Ag-Cu-Ti + Cu mesh/Cu joint was larger. The joints were mainly composed of four parts: Ti_3SiC_2 ceramic, the diffusion and reaction layer in Ti_3SiC_2 ceramic, the filler layer, and copper. Owing to the addition of copper mesh, the thickness of the filler layer in Ti_3SiC_2/Ag-Cu-Ti + Cu mesh/Cu joint was significantly greater than that without copper mesh. Moreover, the increase in the concentration gradient of Cu at the interface led to an increase in the thickness of the diffusion and reaction layer.

From the brazing quality of joints, it was found that a few defects appeared in the brazed joint without copper mesh, resulting from the different thermal expansion coefficients of Ti_3SiC_2 ceramic, the pure copper and the filler layer. Due to the poor plasticity of Ti_3SiC_2 ceramic, the difference in shrinkage during the cooling process led to the high residual stress at the interface of joints, especially the ceramic side. The residual stress concentration and the poor plasticity of ceramic caused the initiation and propagation of cracks. When using the filler with copper mesh, the joint was also influenced by the residual stress due to the same reason. However, the residual stress concentration could be relieved owing to the plastic deformation of copper mesh, effectively reducing the probability of crack initiation.

In order to investigate the diffusion of atoms and products at the interface, the EDS analysis (line scan) across the joint interface and the high-magnification microstructure at the interface are shown in Figure 4c,d. The results of EDS analysis (line scan) show that the elements in filler diffused into the Ti_3SiC_2 ceramic to a certain extent, especially Cu element. In region I, there were only Ti, Si, and C elements, indicating that it was mainly Ti_3SiC_2 ceramic. In region II, there were mainly Ti, Si, C, Cu, and a small amount of Ag

elements. The appearance of Cu and Ag elements can be attributed to the diffusion of atoms at the interface, and the content of Cu and Ag elements gradually decreased as the distance from the interface increased. According to previous research by Wang [39], it was mainly Ti-Si, Ti-C, and Ti -Cu and other intermetallic compounds in region II. In the filler layer (region III), the content of Cu and Ag elements increased and occupied the majority, while that of Ti and Si elements shows a significant decrease. The Cu and Ag elements in region III were derived from Ag-Cu-Ti filler and copper mesh. Region IV only contained Cu element, so it was obviously pure copper base material. From the magnified microstructure of joint, the ceramic is not completely dense and there are some voids. The microstructure in region III was gray-white network structure and had a small amount of dispersed nubby grey products.

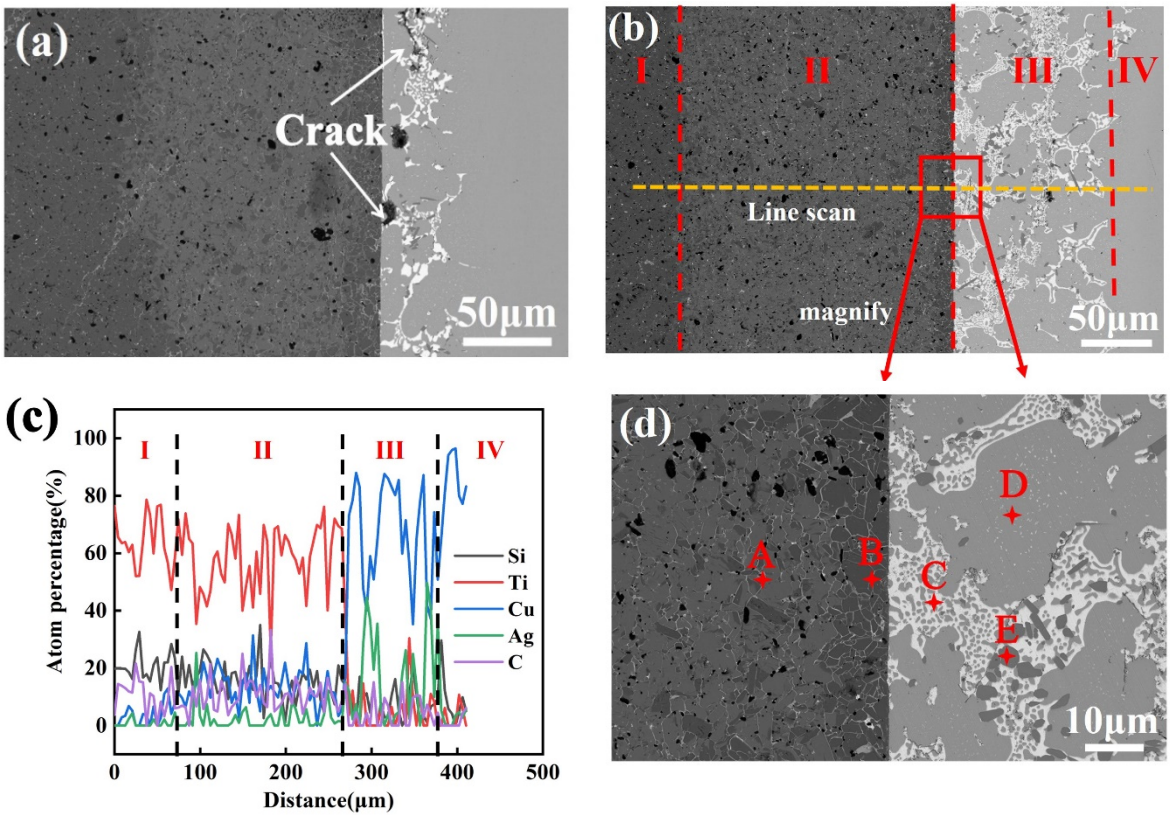

Figure 4. Interfacial microstructure of Ti_3SiC_2/Cu brazed joints using Ag-Cu-Ti filler (**a**) without copper mesh (**b**) with copper mesh at 880 °C for 10 min and (**c**) elemental EDS line profile result in (**b**,**d**) high-magnified image of zone in (**b**).

In order to investigate the distribution of the main elements in the joint in detail, the EDS analysis (surface scanning) of the entire joint was carried out. The surface scanning result of the joint interface with copper mesh is shown in Figure 5. According to the distribution of elements, it can be deduced that the atomic diffusion and chemical reaction between Ti_3SiC_2 ceramic and the fillers was relatively intense, illustrating that the atomic diffusion and reaction were sufficient and could fully guarantee the joint quality. In addition, the copper mesh was not seriously eroded and the framework existed stably as shown in the distribution of Cu in Figure 5d, which provided a guarantee for its plastic deformation to relieve the residual stress of the joint.

In order to determine the elemental composition of the reaction products in the brazed joint obtained using copper mesh, the EDS analysis was carried out on the reaction products at the interface as shown in Figure 4d. Table 2 lists the EDS results of interface products marked in Figure 4d. Moreover, the X-ray diffraction analyzer (XRD) is used to analyze the phase structures of the products at the interface. Because the width of reaction layer was only about 200–300 μm, it was difficult to directly detect and analyze the products owing

to limitation of the instrument. Therefore, the shear fracture of joint was used to detect and analyze the type of products using XRD, and the result is shown in Figure 6.

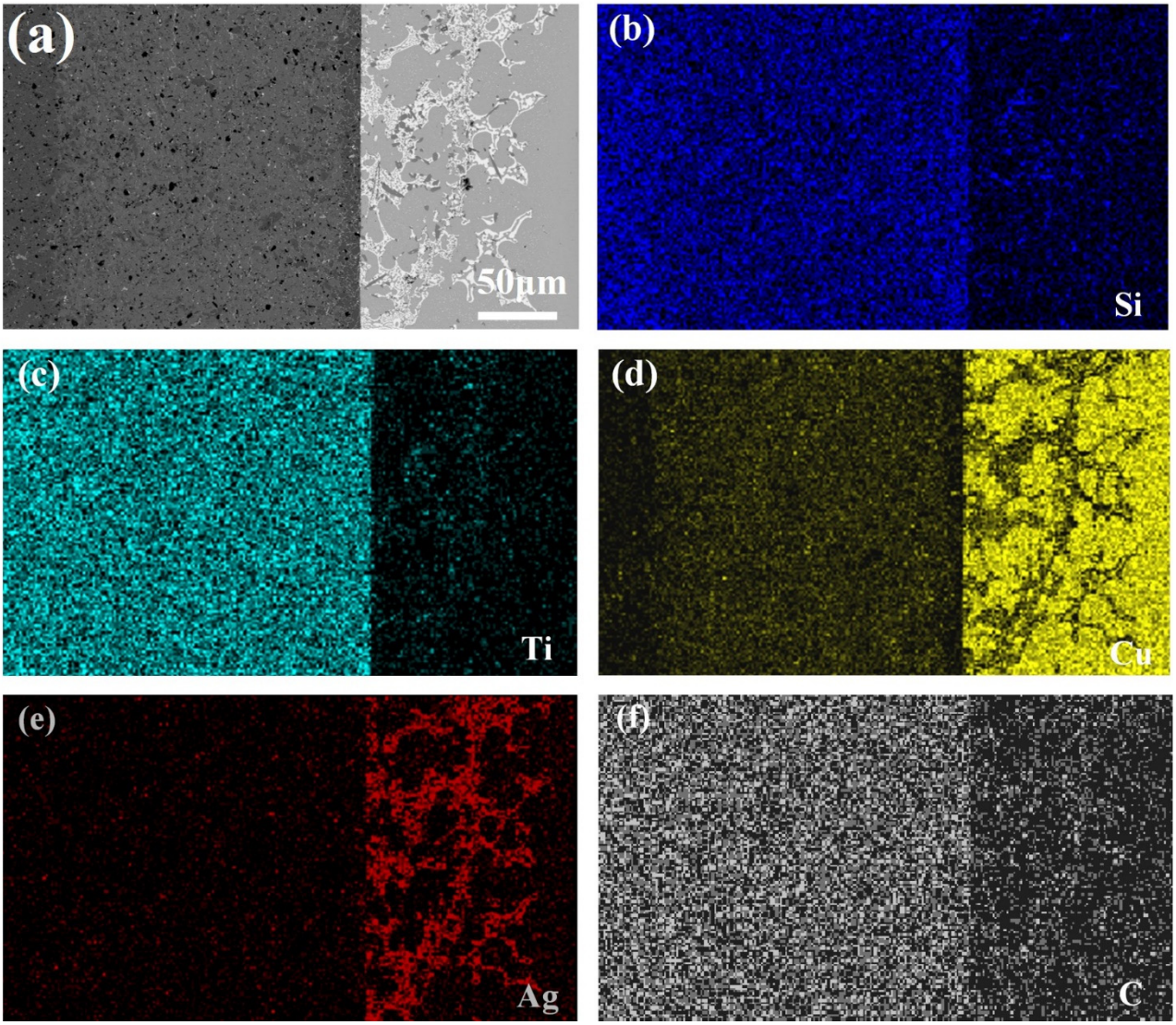

Figure 5. The area of surface scanning (**a**) and EDS maps of (**b**) Si, (**c**) Ti, (**d**) Cu, (**e**) Ag, and (**f**) C.

Table 2. Compositions and possible phases of each spot marked in Figure 4d (at. %).

Products	C	Si	Ti	Cu	Ag	Possible Phases
A	10.31	18.26	63.20	8.23	–	Ti_5Si_3, Ti_3Cu, TiC
B	4.13	30.57	54.07	11.23	–	Ti_5Si_3, Ti_2Cu, TiC
C	2.79	1.38	–	32.96	62.87	Ag-Cu eutectics
D	–	7.06	–	89.77	3.17	Cu (s, s)
E	–	30.45	36.31	31.26	1.98	TiSiCu

According to the results of EDS analysis, the main elements contained in point A and point B were the same, but the content of the elements was slightly different owing to the atomic diffusion between different materials. Under high-temperature conditions, a large amount of free Ag, Cu, and Ti atoms were produced from the molten fillers. The free Ti atoms reacted with Ti_3SiC_2 ceramic, leading to the decomposition of Ti_3SiC_2 ceramic. Owing to the concentration gradient, the atomic diffusion between different materials occurred at the interface. Most obviously, Ag and Cu atoms diffused to Ti_3SiC_2 ceramic side. Moreover, Ti was enriched in the Ti_3SiC_2 ceramic as the holding time increased owing

to its activeness. According to the study from Gu [44] et al., the following three reactions may occur between Ti element and Ti_3SiC_2 ceramic in high-temperature conditions:

$$Ti + Ti_3SiC_2 \rightarrow TiC_X + Ti_5Si_3 + TiSi_2 \quad (1)$$

$$Ti + Ti_3SiC_2 \rightarrow TiC_X + Si + Ti \rightarrow TiC_X + Ti_XSi_Y \quad (2)$$

$$Ti + Ti_3SiC_2 \rightarrow Ti_XSi_Y + C + Ti \rightarrow TiC_X + Ti_XSi_Y. \quad (3)$$

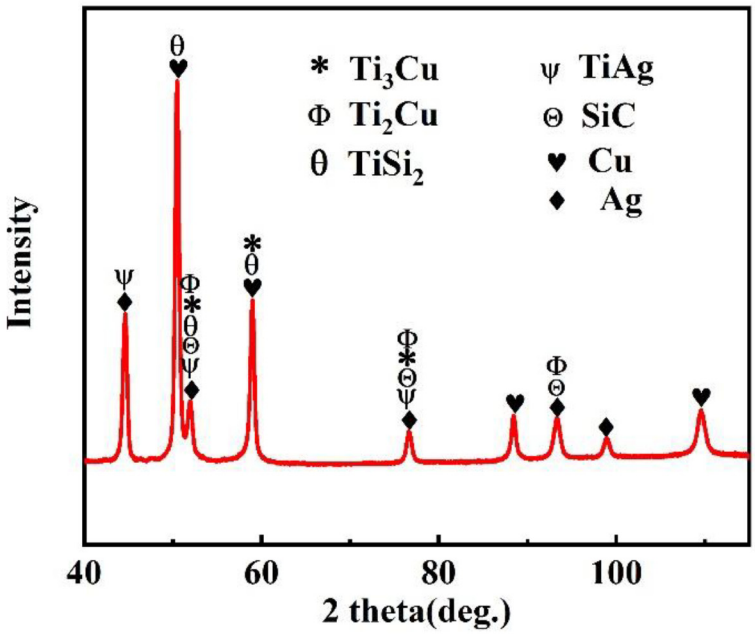

Figure 6. XRD pattern of fracture.

Combined with XRD analysis, EDS point scanning analysis results and the binary alloy phase diagram, it could be inferred that the reaction products of Ti element and Ti_3SiC_2 ceramic were TiC_X, Ti_XCu, and Ti_XSi_Y. Therefore, the reaction products in region II were mainly Ti_5Si_3, Ti_2Cu, Ti_3Cu, and TiC. According to the results of EDS point scanning analysis, the gray-white network structure (point C) mainly contained Ag and Cu atoms with an atomic ratio of about 1.9:1. Combined with the binary alloy phase diagram, it is believed that the gray-white network structure was Ag-Cu eutectic. With the holding time increasing, the erosion of pure copper and copper mesh generated a large amount of Cu atoms in the interface. In addition, the intermetallic compounds formed by the interfacial reaction such as Ti_5Si_3, TiC, Ti_2Cu, and Ti_3Cu prevented the diffusion of Cu as well as Ag atoms into Ti_3SiC_2 ceramic. Therefore, the Ag-Cu eutectic structure was formed due to the combination of free Cu atoms and the free Ag atoms. However, Ag atoms came from the melting of the filler, and the number of atoms was limited. As a result, a large amount of Cu atoms will eventually exist in the form of Cu-based solid solution at the interface. The point E mainly contained Ti, Si, and Cu with the atomic ratio of about 1:1:1, so it is inferred to be TiSiCu ternary intermetallic compound. According to Formula (2), the active Ti atoms reacted with Ti_3SiC_2 ceramic and produced free Ti and Si atoms at the interface, which reacted with a large amount of free Cu atoms at the interface and formed TiSiCu ternary intermetallic compound. Therefore, the main products in region II were Ti_5Si_3, TiC, Ti_2Cu, Ti_3Cu, and other intermetallic compounds, and the microstructure in region III was mainly Cu-based solid solution, Ag-Cu eutectic, and TiSiCu ternary intermetallic compound.

3.2. The Effects of Brazing Parameters on the Microstructure and Mechanical Properties of Joints

The interfacial microstructure of the Ti_3SiC_2 ceramic/Ag-Cu-Ti + Cu mesh/pure copper joints obtained under different brazing temperatures is shown in Figure 7. When the holding time of brazing was constant, the brazing temperature was a variable, which was

set to 840, 860, 880, and 900 °C, respectively. As shown in Figure 7a, the high-temperature fluidity of the filler was poor at 840 °C, resulting in the difficulty in filling the voids of copper mesh and the gap between ceramic and pure copper at the relatively low brazing temperature. Therefore, many voids and other defects appeared at the interface. With the temperature rising, the fluidity of the liquid filler was improved and the defects resulting from poor liquidity at the interface disappeared gradually. Due to the erosion and diffusion of more atoms in the ceramic and pure copper, the reaction layer gradually became thicker. At the same time, the gray-white networked Ag-Cu eutectic structure began to gradually disperse. When the brazing temperature reached to 880 °C, the defects disappeared completely and the interface structure was greatly improved.

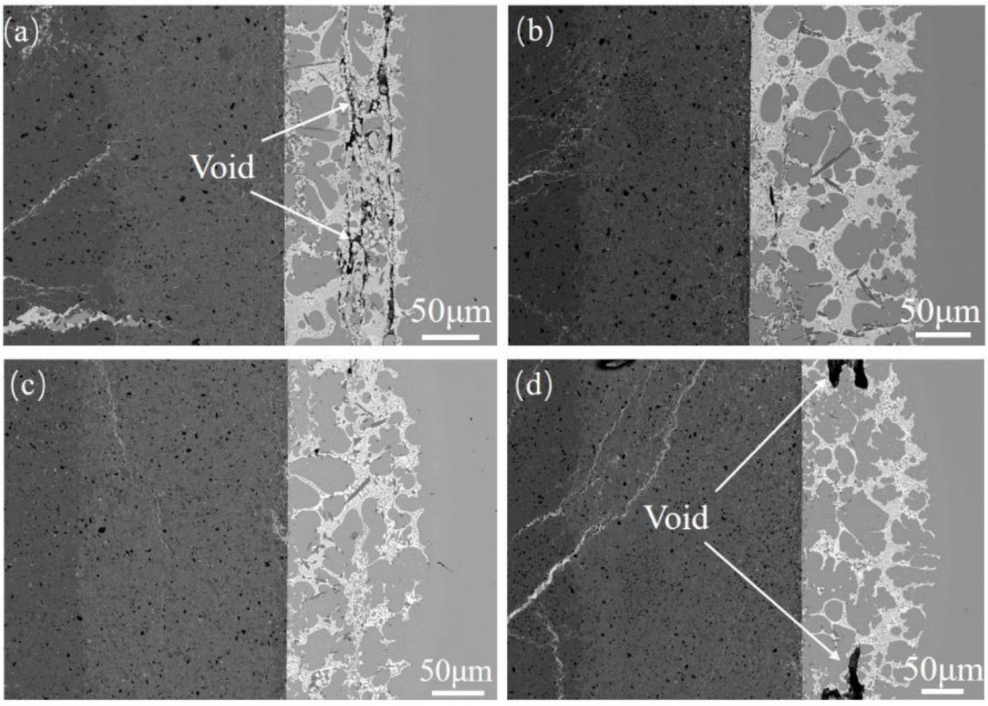

Figure 7. Effect of brazing temperature on interfacial microstructure of Ti_3SiC_2/Ag-Cu-Ti + Cu mesh/Cu joints: (**a**) T = 840 °C, (**b**) T = 860 °C, (**c**) T = 880 °C, and (**d**) T = 900 °C.

However, as the brazing temperature further increased and reached to 900 °C, many defects such as voids appeared at the interface again due to Kirkendall effect. There were huge differences in the atomic diffusion rate between pure copper and Ti_3SiC_2 ceramic especially in excessively high temperature. The difference caused more Ag and Cu atoms diffused into the Ti_3SiC_2 ceramic side, while less Ti and Si atoms diffused from Ti_3SiC_2 ceramic side into the filler layer and pure copper side, resulting in the generation of numerous voids in the copper side. Meanwhile, the brittleness of the intermetallic compounds caused poor toughness and led to voids in the joint. Due to the high temperature, the differences of CTE between Ti_3SiC_2 ceramic and pure copper were more obvious, which led to larger difference of shrinkage between the brazing materials in the cooling process. Thus, there were more voids and other defects at the interface when using the brazing temperature of 900 °C.

Besides studying the effects of brazing temperature, the effects of holding time on the microstructure were also investigated. Figure 8 shows the magnified interfacial microstructure of Ti_3SiC_2/Ag-Cu-Ti + Cu mesh/Cu joints obtained using holding times of 5, 10, 20, and 30 min, respectively, while the brazing temperature was constant at 870 °C.

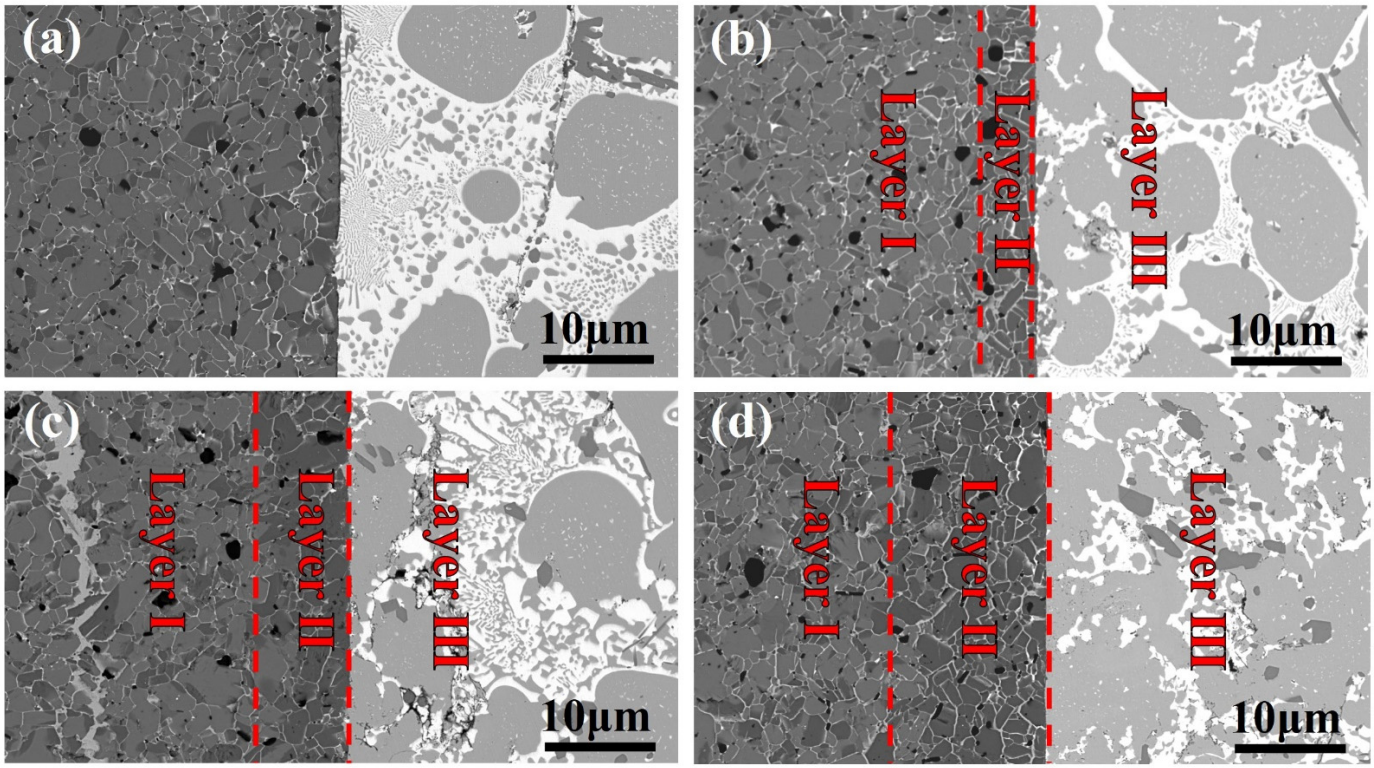

Figure 8. Effects of holding time on interfacial microstructure of Ti_3SiC_2/Ag-Cu-Ti + Cu mesh/Cu brazed joints: (**a**) t = 5 min, (**b**) t = 10 min, (**c**) t = 20 min, and (**d**) t = 30 min.

As shown in Figure 8, when the holding time was 5 min, the relatively straight interface between the filler and the Ti_3SiC_2 ceramic/copper base material indicated that the atomic diffusion was insufficient resulting in a clear interface between the filler and the base materials. With the holding time increasing, an obvious reaction layer appeared in the Ag-Cu-Ti/Ti_3SiC_2 ceramic interface (for easy observation, the reaction layer is marked with reaction layers I, II, and III in Figure 8), the thickness of which increased with the holding time increasing. The Ti atoms in the filler metal were enriched on the ceramic matrix side and begin to react with it to form various intermetallic compounds. The reaction layer I is mainly formed by intermetallic compounds such as Ti_5Si_3, TiC, and Ti_2C as shown in the reaction layer I of Figure 8. As the holding time continued to increase, the side interface products became more and more complex, caused by the active element Ti in the Ag-Cu-Ti filler. As mentioned above, the diffusion distance of Ti atoms in the brazing filler metal gradually accumulates on the Ti_3SiC_2 ceramic substrate side and reacted with it to form Ti-Si, Ti-C, Ti-Cu, and other intermetallic compounds as the holding time increased. With the extension of the holding time, the phase composition of the compound was different. As shown in the reaction layer II in Figure 8, the phase composition is Ti_5Si_3, TiC and Ti_3Cu. With the formation of many intermetallic compounds, the continuous diffusion of Cu atoms at the interface to the Ti_3SiC_2 ceramic was hindered. As the copper mesh and the copper matrix continued to be eroded with the extension of the holding time, leading to the generation of amounts of free Cu atoms at the interface, which reacted with the Ag atoms from the filler to form the Ag-Cu eutectic structure, as shown in the white network reaction layer III of Figure 8. In short, when the Ag-Cu-Ti metallic filler is melted, the liquid filler separates into two liquid phases, the Ag-rich phase and the Cu/Ti compound-rich phase [45]. The presence of Ag will promote the separation of Ti from the Ti/Cu compound, thus increasing the activity of the Ag-Cu-Ti filler brazing ceramic materials [46]. As the holding time increased, the diffusion of atoms becomes more and more sufficient. The presence of Ag atoms promoted the separation of Ti atoms from the Ti/Cu compounds. Ti atoms diffused and segregated on the Ti_3SiC_2 ceramic side, due to its higher activity,

reacting with Ti_3SiC_2 ceramic to produce Ti_5Si_3, TiC, Ti_2Cu, Ti_3Cu, and other intermetallic compounds. Ag atoms reacted with many free Cu atoms at the interface to form Ag-Cu eutectic structure. Since the Ag atoms at the interface came from the Ag-Cu-Ti metal filler, the solidification process was not supplemented. Therefore, some Cu atoms reacted with Ti and Si to form TiSiCu ternary intermetallic compounds. At the same time, the excess Cu atoms were precipitated as the form of the matrix solid solution structure at the interface.

It can be drawn from the analysis of microstructure that the brazing temperature and holding time have significant effects on the interfacial microstructure of the brazed joint, including the thickness of the reaction layer at the interface and the microstructure of solid solution, which affect the mechanical properties finally.

As shown in Figure 9a, as the temperature rose from 840 to 900 °C, the shear strength value of the joints first increased and then decreased, reaching to the maximum value of 62.2 ± 1.5 MPa when the temperature is at 880 °C. As analyzed previously, at a lower temperature of 840 °C, the defects such as microscopic voids caused by uncomplete melting of filler metal at the interface directly led to the lower shear strength of the joint. With the rising of temperature, the filler metal completely melts, which is beneficial to the wetting of Ti_3SiC_2 ceramic. Therefore, a good metallurgical bond was formed at the interface, and the defects gradually disappeared. When the temperature rose to 880 °C, the interfacial structure of the joint was dense and complete without any defect. At this time, the shear strength value of the joint reached to the maximum value of 62.2 ± 1.5 MPa. However, when the temperature increased further and reached to 900 °C, the shear strength value of the brazed joint dropped sharply, which was only 38.3 ± 1.3 MPa, 62.4% lower than the peak value. This was caused by the increasing difference of CTE between base materials and many intermetallic compounds from excessive diffusion and reaction of atoms in high temperature conditions. Therefore, in order to ensure the fine interfacial microstructure and mechanical property of the brazed joint, the brazing temperature should be controlled between 860 and 880 °C.

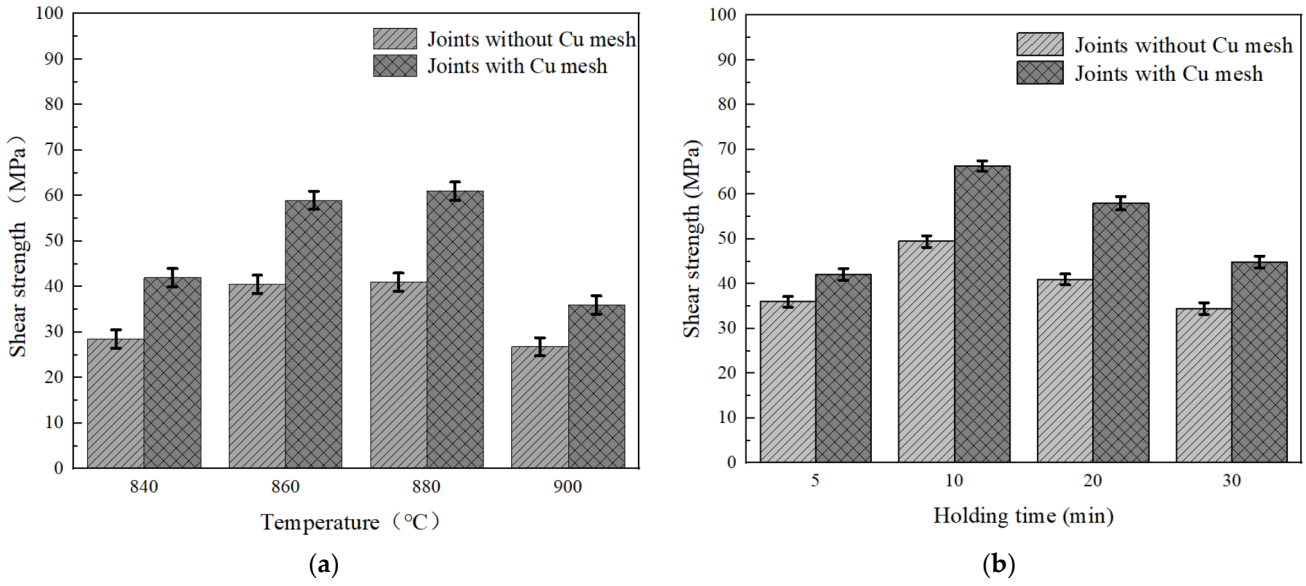

Figure 9. The compassion of mechanical property between the brazed joints with and without copper mesh under different brazing parameters: (**a**) the condition with the same holding time and different brazing temperature and (**b**) the condition with the same temperature and different holding time.

The effect of holding time on the shear strength of brazed joint at the brazing temperature of 870 °C is shown in Figure 9b and the holding time used in each experiment was 5, 10, 20, and 30 min. As shown in Figure 9b, with the holding time promoted from 5 to 30 min, the shear strength of the joint showed a trend of first increasing and then decreasing, and the shear strength value reached to the maximum value of 66.3 ± 1.2 MPa when the condi-

tion is at the temperature of 870 °C and for 10-min holding time. As discussed previously, when the holding time was 5 min, the joint shear strength was only 42.1 ± 1.3 MPa owing to the uncomplete melting of filler metal and insufficient reaction. With the promotion of the holding time, the brazing filler metal completely melted and violent reaction occurred, forming a metallurgical reaction layer, which led to the tightly bonded joint and the increasing of shear strength. However, the thickness of the reaction layer composed of intermetallic compounds increased with the further promotion of holding time, increasing the brittleness of the joint interface, generating the defects such as cracks, and deteriorating the performance of the joint. The shear strength of the joint decreased from 66.3 ± 1.2 MPa after the holding time for 10 min to 58 ± 1.5 MPa. When the holding time was promoted to 30 min, the thickness of the intermetallic compounds reaction layer reached to the maximum value, and the intergranular infiltration also increases, resulting in the joint with shear strength of only 44.9 ± 1.3 MPa, which was only 67.7% of the peak value.

In summary, it can be drawn that with brazing temperature and holding time increasing, the metallurgical bonding of interface was densified, the number of voids decreased at the interface, and the increasement of the thickness of reaction layer was unobvious, resulting in the promotion of sheer strength, which reached to the maximum value of 66.3 ± 1.2 MPa at 870 °C for 10 min. The shear strength decreased after the further increasing of temperature and holding time owing to the excessively thick reaction layer of intermetallic compounds.

4. Conclusions

The brazing of Ti_3SiC_2 ceramic and Cu was successfully achieved using Ag-Cu-Ti filler with copper mesh. The interfacial microstructure and prosperities of Ti_3SiC_2/Ag-Cu-Ti + Cu mesh/Cu joints were investigated in details and compared with the joint without copper mesh. Meanwhile the optimal brazing parameter was also obtained in this study. The main conclusions can be summarized as follows.

1. A sound joint was successfully achieved at 880 °C for 10 min with Ag-Cu-Ti + Cu mesh fillers. The typical interfacial microstructure of joint was Ti_3SiC_2 ceramic/ Ti_5Si_3 + TiC + Ti_2Cu + Ti_3Cu/Cu (s, s)/eutectic Ag-Cu + TiSiCu/Cu.
2. With the rising of brazing temperature and the extension of holding time, Ti atoms diffused and gathered on the Ti_3SiC_2 ceramic side, reacting with it to result in intermetallic compounds. The Cu atoms from the copper mesh and pure Cu partially eroded into the liquid metal filler and diffused into the Ti_3SiC_2 ceramic, reacting with it to generate a reaction layer of Ti-Cu intermetallic compounds, which blocked the diffusion of Cu atoms at the interface, causing the generation of Cu solid solution tissue; in addition, the remaining Cu atoms reacted with the free Ag atoms to generate Ag-Cu eutectic structure.
3. Compared with the value for the condition without copper mesh, the shear strength of joint brazed at 870 °C for 10 min was calculated to 66.3 ± 1.2 MPa, promoted about 34.7%. This is due to the extraordinary plasticity of copper mesh and the liquid filler diverted by copper mesh, releasing the residual stress caused by the different CTE of base materials. Meanwhile the diffusion of atom was partially inhibited by copper mesh, resulting in the decrease of intermetallic compounds, improving the microstructure and enhancing mechanical properties.
4. With brazing temperature and holding time increasing, the metallurgical bonding of interface was densified, the number of voids decreased at the interface, and the increasement of the thickness of reaction layer was unobvious, resulting in the promotion of sheer strength, which reached to the maximum value of 66.3 ± 1.2 MPa at 870 °C for 10 min. The shear strength decreased after the further increasing of temperature and holding time owing to the excessively thick reaction layer of intermetallic compounds.

Author Contributions: Conceptualization, H.C. and D.L.; investigation, S.Z. and D.L.; resources, Z.S. and W.L.; data curation, H.C. and X.N.; writing—original draft preparation, X.N. and D.L.; writing—review and editing, H.C. and X.N.; project administration, Z.S., W.L. and J.C.; funding acquisition, H.C. All authors have read and agreed to the published version of the manuscript.

Funding: This research was funded by the National Natural Science Foundation of China (Grant No. 51974260 and No. 51775442), Natural Science Basic Research Plan in Shaanxi Province of China (Program No. 2018JZ5009), and State Key Laboratory of Advanced Welding and Joining in Heilongjiang Province of China (Pro-gram No. AWJ-20-M13).

Institutional Review Board Statement: Not applicable.

Informed Consent Statement: Not applicable.

Data Availability Statement: Not applicable.

Acknowledgments: Authors gratefully acknowledge the financial support from the National Natural Science Foundation of China (Grant No. 51974260 and No. 51775442), Natural Science Basic Research Plan in Shaanxi Province of China (Program No. 2018JZ5009), and State Key Laboratory of Advanced Welding and Joining in Heilongjiang Province of China (Program No. AWJ-20-M13).

Conflicts of Interest: The authors declare no conflict of interest.

References

1. Daoudi, B.; Yakoubi, A.; Beldi, L.; Bouhafs, B. Full-potential electronic structure of Hf_2AlC and Hf_2AlN. *Acta Mater.* **2007**, *55*, 4161–4165. [CrossRef]
2. Barsoum, M.W.; Farber, L.; El-Raghy, T. Dislocations, kink bands, and room-temperature plasticity of Ti_3SiC_2. *Metall. Mater. Trans. A* **1999**, *30*, 1727–1738. [CrossRef]
3. Hadji, Y.; Haddad, A.; Yahi, M.; Benamar, M.E.A.; Miroud, D.; Sahraoui, T.; Hadji, M.; Barsoum, M.W. Joining Ti_3SiC_2, MAX phase with 308 stainless steel and aluminum fillers by tungsten inert gas (TIG)-brazing process. *Ceram. Int.* **2016**, *42*, 1026–1035. [CrossRef]
4. Dezellus, O.; Gardiola, B.; Andrieux, J.; Lay, S. Experimental evidence of copper insertion in a crystallographic structure of Ti_3SiC_2 MAX phase. *Scr. Mater.* **2015**, *104*, 17–20. [CrossRef]
5. Xie, H.; Ngai, T.L.; Zhang, P.; Li, Y.Y. Erosion of Cu-Ti_3SiC_2 composite under vacuum arc. *Vacuum* **2015**, *114*, 26–32. [CrossRef]
6. Chen, H.Y.; Peng, J.K.; Fu, L. Effects of interfacial reaction and atomic diffusion on the mechanical property of Ti_3SiC_2, ceramic to Cu brazing joints. *Vacuum* **2016**, *130*, 56–62. [CrossRef]
7. Dang, W.T.; Ren, S.F.; Zhou, J.S.; Yu, Y.J.; Li, Z.; Wang, L.Q. Influence of Cu on the mechanical and tribological properties of Ti_3SiC_2. *Ceram. Int.* **2016**, *42*, 9972–9980. [CrossRef]
8. Deng, Z.X.; Gingerich, M.B.; Han, T.Y.; Dapino, M. Yttria-stabilized zirconia-aluminum matrix composites via ultrasonic additive manufacturing. *Compos. Part B Eng.* **2018**, *151*, 215–221. [CrossRef]
9. Wahba, M.; Mizutani, M.; Katayama, S. Single pass hybrid laser-arc welding of 25 mm thick square groove butt joints. *Mater. Des.* **2016**, *97*, 1–6. [CrossRef]
10. He, P.; Zhang, J.; Zhou, R.; Li, X.Q. Diffusion bonding technology of a titanium alloy to a stainless steel web with an Ni interlayer. *Mater. Charact.* **1999**, *43*, 287–292. [CrossRef]
11. Song, C.B.; He, P.; Lin, T.S.; Wei, H.M.; Yang, W.Q. Electroplating assisted diffusion bonding of ZrC-SiC composite for full ceramic joints. *Ceram. Int.* **2014**, *40*, 7613–7616. [CrossRef]
12. Xu, X.Y.; Xu, X.H.; Wu, J.F.; Lao, X.B. Fabrication and characterization of cordierite-based glass-ceramic adhesives for bonding solar heat transmission pipelines. *Ceram. Int.* **2017**, *43*, 149–156.
13. Lan, L.; Yu, J.B.; Yang, Z.G.; Li, C.J.; Ren, Z.M.; Wang, Q.L. Interfacial microstructure and mechanical characterization of silicon nitride/nickel-base superalloy joints by partial transient liquid phase bonding. *Ceram. Int.* **2016**, *42*, 1633–1639. [CrossRef]
14. Cui, B.; Huang, J.H.; Cai, C.; Chen, S.H.; Zhao, X.K. Microstructures and mechanical properties of Cf/SiC composite and TC4 alloy joints brazed with (Ti-Zr-Cu-Ni) + W composite filler materials. *Compos. Sci. Technol.* **2014**, *97*, 19–26. [CrossRef]
15. Avettand-Fènoël, M.-N.; Naji, K.; Poulignyb, P. Brazing vs. diffusion welding of graded Fe based matrix composite and yttria stabilized zirconia. *J. Manuf. Process.* **2019**, *45*, 557–570. [CrossRef]
16. Chen, X.G.; Liu, L.; Yan, J.C.; Zou, G.S. Interfacial structure and formation mechanism of ultrasonic-assisted brazed joint of SiC ceramic and with Al-12Si filler metals in air. *J. Mater. Sci. Technol.* **2017**, *33*, 492–498. [CrossRef]
17. Chen, X.G.; Yan, J.C.; Ren, S.C.; Wang, Q.; Wei, J.H.; Fan, G.H. Microstructure, mechanical properties, and bonding mechanism of ultrasonic-assisted brazed joints of SiC ceramics with ZnAlMg filler metals in air. *Ceram. Int.* **2014**, *40*, 683–689. [CrossRef]
18. Shi, J.M.; Feng, J.C.; Tian, X.Y.; Liu, H.; Zhang, L.X. Interfacial microstructure and mechanical property of ZrC-SiC ceramic and Ti6Al4V joint brazed with Ag-Cu-Ti alloy. *J. Eur. Ceram. Soc.* **2017**, *37*, 2769–2778. [CrossRef]
19. Ren, H.S.; Xiong, H.P.; Long, W.M.; Shen, Y.X.; Pang, S.J.; Chen, B.; Cheng, Y.Y. Interfacial diffusion reactions and mechanical properties of Ti3Al/Ni-based superalloy joints brazed with AgCuPd filler metal. *Mater. Charact.* **2018**, *144*, 316–324. [CrossRef]

20. Waetzig, K.; Schilm, J.; Mosch, S.; Tillmann, W.; Eilers, A.; Wojarski, L. Influence of the brazing paste composition on the wetting behavior of reactive air brazed metal–ceramic joints. *Adv. Eng. Mater.* **2021**, *32*, 2000711. [CrossRef]
21. Qiu, Q.W.; Wang, Y.; Yang, Z.W.; Wang, D.P. Microstructure and mechanical properties of Al_2O_3 ceramic and Ti6Al4V alloy joint brazed with inactive Ag-Cu and Ag-Cu+B. *J. Eur. Ceram. Soc.* **2016**, *36*, 2067–2074. [CrossRef]
22. Pietrzak, K.; Kaliński, D.; Chmielewski, M. Interlayer of Al_2O_3-Cr functionally graded material for reduction of thermal stresses in alumina-heat resisting steel joints. *J. Eur. Ceram. Soc.* **2007**, *27*, 1281–1286. [CrossRef]
23. Song, X.G.; Zhao, Y.X.; Hu, S.P.; Cao, J.; Fu, W.; Feng, J.C. Wetting of Ag-Cu-Ti filler on porous Si_3N_4 ceramic and brazing of the ceramic to TiAl alloy. *Ceram. Int.* **2018**, *44*, 4622–4629. [CrossRef]
24. Yang, M.; Lin, T.; He, P.; Huang, Y.D. In situ synthesis of TiB whisker reinforcements in the joints of Al_2O_3/TC4 during brazing. *Mater. Sci. Eng. A* **2011**, *528*, 3520–3525. [CrossRef]
25. Song, X.G.; Cao, J.; Wang, Y.F.; Feng, J.C. Effect of Si_3N_4 Particles addition in Ag-Cu-Ti filler alloy on Si_3N_4/TiAl brazed joint. *Mater. Sci. Eng. A* **2011**, *528*, 5135–5140. [CrossRef]
26. Wang, T.P.; Ivas, T.; Leinenbach, C.; Zhang, J. Microstructural Characterization of Si_3N_4/42CrMo Joint Brazed with Ag-Cu-Ti + TiNp Composite Filler. *J. Alloy. Compd.* **2015**, *651*, 623–630. [CrossRef]
27. Wang, T.P.; Zhang, J.; Liu, C.F.; Wang, G.C. Microstructure and Mechanical Properties of Si_3N_4/42CrMo Joints Brazed with TiNp Modified Active Filler. *Ceram. Int.* **2014**, *40*, 6881–6890. [CrossRef]
28. Song, X.R.; Li, H.J.; Casalegno, V.; Savol, M.; Ferraris, M.; Zeng, X.R. In situ TiC Particle Reinforced TiCuZrNi Brazing Alloy for Joining C/C Composites to Ti6Al4V. *Int. J. Appl. Ceram. Technol.* **2018**, *15*, 611–618. [CrossRef]
29. Song, X.R.; Li, H.J.; Casalegno, V.; Savol, M.; Ferraris, M.; Zeng, X.R. Microstructure and Mechanical Properties of C/C Composite/Ti6Al4V Joints with a Cu/TiCuZrNi Composite Brazing Alloy. *Ceram. Int.* **2016**, *42*, 6347–6354. [CrossRef]
30. Guo, W.; Gao, T.F.; Cui, X.F.; Zhu, Y.; Chu, P.K. Interfacial Reactions and Zigzag Groove Strengthening of C/C Composite and Rene N5 Single Crystal Brazed Joint. *Ceram. Int.* **2015**, *41*, 11605–11610. [CrossRef]
31. Chang, H.; Park, S.; Choi, S.; Kim, T. Effects of Residual Stress on Fracture Strength of Si_3N_4/Stainless Steel Joints with a Cu Interlayer. *Mater. Eng. Perform.* **2002**, *11*, 640–644. [CrossRef]
32. Morales-Péreza, M.; Ceja-Cárdenas, L. Interfacial characterization in the brazing of silicon nitride to niobium joining using a double interlayer. *Mater. Charact.* **2017**, *131*, 316–323. [CrossRef]
33. Zhao, Y.T.; Wang, Y.; Yang, Z.W.; Wang, D.P. Relief of Residual Stress in Al_2O_3/Nb Joints Brazed with Ag-Cu-Ti/Cu/Ag-Cu-Ti Composite Interlayer. *Arch. Civ. Mech. Eng.* **2019**, *19*, 1–10. [CrossRef]
34. Yang, Z.W.; Zhang, L.X.; Chen, Y.C.; Qi, J.L.; He, P.; Feng, J.C. Interlayer design to control interfacial microstructure and improve mechanical properties of active brazed Invar/SiO_2-BN joint. *Mater. Sci. Eng. A* **2013**, *575*, 199–205. [CrossRef]
35. Shirzadi, A.A.; Zhu, Y.; Bhadeshia, H.K.D.H. Joining ceramics to metals using metallic foam. *Mater. Sci. Eng. A* **2008**, *496*, 501–506. [CrossRef]
36. Junga, A.; Luksch, J.; Diebels, S.; Schäfer, F.; Motz, C. In-situ and ex-situ microtensile testing of individual struts of Al foams and Ni/Al hybrid foams. *Mater. Des.* **2018**, *153*, 104–119. [CrossRef]
37. Feng, M.N.; Xie, Y.; Zhao, C.F.; Luo, Z. Microstructure and mechanical performance of ultrasonic spot welded open cell Cu foam/Al joint. *J. Manuf. Process.* **2018**, *33*, 86–95. [CrossRef]
38. Sun, Z.; Zhang, L.X.; Chang, Q.; Zhang, Z.H.; Hao, T.D.; Feng, J.C. Active brazed Invar-SiO_2f/SiO_2 joint using a low-expansion composite interlayer. *Mater. Process. Technol.* **2018**, *255*, 8–16. [CrossRef]
39. Sun, R.J.; Zhu, Y.; Guo, W.; Peng, P.; Li, L.H.; Zhang, Y.; Fu, J.; Li, F.; Zhang, L.X. Microstructural evolution and thermal stress relaxation of Al_2O_3/1Cr18Ni9Ti brazed joints with nickel foam. *Vacuum* **2018**, *148*, 18–26. [CrossRef]
40. Zaharinie, T.; Moshwan, R.; Yusof, F.; Hamdi, M.; Ariga, T. Vacuum brazing of sapphire with Inconel 600 using Cu/Ni porous composite interlayer for gas pressure sensor application. *Mater. Des.* **2014**, *54*, 375–381. [CrossRef]
41. Tian, X.Y.; Feng, J.C.; Shi, J.M.; Li, H.W.; Zhang, L.X. Brazing of ZrB_2-SiC-C ceramic and GH99 superalloy to form reticular seam with low residual stress. *Ceram. Int.* **2015**, *41*, 145–153. [CrossRef]
42. Wang, Z.Y.; Li, M.N.; Ba, J.; Ma, Q.; Fan, Z.Q.; Lin, J.H.; Zhong, Z.X.; Qi, J.L.; Cao, J.; Feng, J.C. In-Situ synthesized TiC nano-flakes reinforced C/C composite-Nb brazed joint. *J. Eur. Ceram. Soc.* **2018**, *38*, 1059–1068. [CrossRef]
43. Singh, M.; Smith, C.E.; Asthana, R.; Gyekenyesi, A.L. Active metal brazing of graphite foam-to-titanium joints made with SiC-Coated foam. *J. Eur. Ceram. Soc.* **2020**, *40*, 2533–2541. [CrossRef]
44. Gu, W.L.; Zhou, Y.C. Reactions between Ti and Ti_3SiC_2 in temperature range of 1273–1573 K. *Trans. Nonferrous Met. Soc. China* **2006**, *16*, 1288. [CrossRef]
45. Xiong, J.H.; Huang, J.H.; Zhang, H.; Zhao, X.K. Brazing of carbon fiber reinforced SiC composite and TC4 using Ag-Cu-Ti active brazing alloy. *Mater. Sci. Eng. A* **2010**, *527*, 1096–1101. [CrossRef]
46. Mandal, S.; Ray, A.K. Correlation between the mechanical properties and the microstructural behaviour of Al_2O_3-(Ag-Cu-Ti) brazed joints. *Mater. Sci. Eng. A* **2004**, *383*, 235–244. [CrossRef]